Hindawi
Journal of Sensors
Volume 2021, Article ID 6628073, 15 pages
https://doi.org/10.1155/2021/6628073

Research Article

Design of Variable Damping INS for Ships Based on the Variation of Reference Velocity Error

Chuang Liu, Qiuping Wu, Peida Hu, and Rong Zhang

Department of Precision Instrument, Tsinghua University, Beijing 100084, China

Correspondence should be addressed to Qiuping Wu; wuqiuping@mail.tsinghua.edu.cn

Received 17 December 2020; Revised 12 February 2021; Accepted 17 February 2021; Published 26 February 2021

Academic Editor: Carlos Michel

Schuler oscillation damping is one of the key technologies to improve the long-term precision of inertial navigation systems (INSs). Generally, a ship introduces the reference velocity to work on the external horizontal damping status to avoid the effects caused by maneuvers. However, the navigation accuracy is sensitive to the reference velocity error which will be affected by sea conditions and the ship's maneuver. It is necessary to adjust the damping status dynamically as the change of the reference velocity error to ensure the accuracy and stability of INS. To address this problem, a novel variable damping system based on the variation of the reference velocity error is designed in this paper. First of all, this proposed method switched the damping status according to the variation of the reference velocity error in a certain period of time based on the principle of window detection. In addition, this paper designed a fuzzy controller to avoid the overshoot caused by the frequent switching of the damping status. What is more, a method of overshoot suppression was applied in this system. Simulation experiments were conducted to validate the theoretical analysis and the effectiveness of this method. Compared with the undamping system, constant damping system, and traditional variable damping system, the simulation results verified that the designed variable damping system can attenuate the system error caused by reference velocity error most effectively, thus improving the navigation accuracy of INS.

1. Introduction

INSs are widely employed in both military and civilian fields due to their numerous advantages. Compared with satellite navigation systems and radio navigation systems, INSs are completely autonomous navigation systems which have strong independence and good concealment and are invulnerable to external interference [1]. They use accelerometers and gyroscopes to get the acceleration and angular velocity to calculate the position, velocity, and attitude of carriers [2]. Because of the working principle of INS, the system has three kinds of periodic oscillation errors, i.e., the Schuler period, Earth period, and Foucault period error. The amplitudes of these periodic oscillation errors are not attenuated and will continue to accumulate with time on account of the effects of gyroscope drift [3, 4]. For the long-term INS, its navigation accuracy will be greatly affected by these periodic errors. Therefore, to ensure the accuracy of INS, a damping correction network is added to turn INS into a stable system [5, 6].

However, adding a damping correction network breaks the Schuler damping loop so that the accuracy of INS will be affected by the carrier's maneuver [7]. Therefore, INSs primarily work on the external horizontal damping status to compensate the system error caused by the maneuver of ships [8]. For the external horizontal damping system, the reference velocity obtained by electromagnetic velocity log (EML) or Doppler velocity log (DVL) is introduced to the system [9–11]. Yet the accuracy of reference velocity will be affected by the sea conditions and the ship's maneuver, and the navigation accuracy is sensitive to reference velocity error. Reference [12] modeled the velocity error of DVL and analyzed the effect on the external horizontal damping system in detail. To diminish the influence caused by the reference velocity error, a novel horizontal damping network for INS based on complementary filtering was proposed in Reference [13]. In Reference [14], a Kalman filter according to the grid SINS error model which applies to the ship was established to dampen the Schuler periodic oscillation. Reference [15, 16] came up with a novel method which

uses Kalman filtering and feedback calibration to dampen the Schuler oscillation of INS by observing the difference between INS' velocity and EML's or GPS's velocity. The integration INS-DVL algorithm based on the extended Kalman filter was introduced in Reference [17]. Reference [18] proposed an INS/EML integrated navigation system with state-delay Kalman filter. A SINS/DVL integrated positioning system based on adaptive filtering technology is reported in Reference [19]. Reference [20] put forward a DVL-based vehicle velocity solution by using the measured partial raw data of DVL and additional information, thereby deriving an extended loosely coupled approach. Reference [21] changed the traditional damping network structure and carried out a method to design the parameters of damping a network quickly with external velocity.

To improve the accuracy of the navigation system, it is necessary to design variable damping INS and suppress the overshoot of the damping switch. Mandour and El-Dakiky studied the optimal damping network and gave three forms of the damping network with the optimal value of each coefficient [22]. In Reference [23], the choice principle, optimal second-order horizontal damping network, and parameters of an optimal damping network were discussed. Then, this paper designed a variable coefficient horizontal damping network to improve the navigation accuracy. Reference [24] added three different types of damping feedback in three loops and made use of its own velocity information to compensate errors. In Reference [25–27], in accordance with the magnitude of motion acceleration, a method of adjusting the damping network parameters adaptively to make the system error minimum was given. To suppress the overshoot when the working status of INS is switched, a double model based on INS damping overshoot error suppression algorithm was proposed in Reference [28]. Reference [29] designed a second-order variable damping network where a fuzzy controller was used to determine the current motion status. In order to simplify the design of the traditional damping network and suppress its overshoot errors while switching status, a continuously adjustable internal horizontal damping method using a proportional control was proposed in Reference [30]. Reference [31] presented a method of adaptive robust damping of oscillations in the gyroaccelerometer system. An adaptive control method to adjust its parameters in real time with the change of sea condition was presented in Reference [32].

Although there are a lot of methods to reduce the influence of the reference velocity error on system accuracy, they are not suitable when the reference velocity error is large for a long time. Besides, adjusting the damping status or damping coefficient will result in overshoot error. Aiming at the shortcomings of traditional horizontal damping method, a novel external horizontal variable damping method based on the variation of reference velocity error is proposed in this paper. First, a reference velocity obtained by EML was introduced to the system to compensate for the system error caused by the ship's maneuver. Then, in view of the limitations of a first-order or second-order horizontal damping network, a high-order system based on the complementary filtering was applied. According to the analysis of the influence of reference velocity error on INS accuracy, this paper designed a variable damping system which switches the damping status based on the variation of the reference velocity error. In this way, the damping status was adjusted in real time to keep the system errors caused by the reference velocity error to a minimum. In order to avoid the switch of damping status frequently, this paper designed a fuzzy controller by using the principle of window detection. In addition, this paper presented a method to suppress the switch overshoot. Compared with a constant damping network and traditional variable damping network, the simulation results demonstrate that the proposed algorithm can suppress the error caused by reference velocity error most effectively and has higher navigation accuracy.

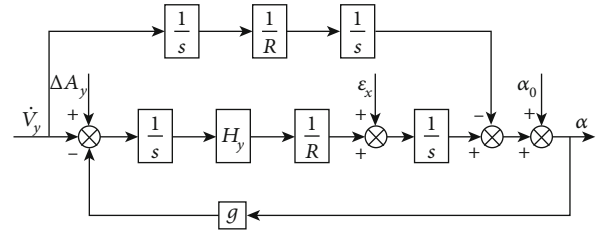

Figure 1: Block diagram of north-level correction circuit (internal damping) [1].

This paper is organized as follows: Section 1 is the introduction. The traditional internal horizontal damping network, external horizontal damping network, and complementary filtering horizontal damping network are reviewed briefly in Section 2. Section 3 describes the novel variable damping INS method proposed in this paper. The simulation experiments and results are presented in Section 4. Section 5 summarizes the conclusion.

2. Traditional Horizontal Damping Network

2.1. Traditional Internal Horizontal Damping Network. If we take the horizontal correction circuit of a single-channel INS (north-level correction circuit of INS) as an example, the horizontal loop model is shown in Figure 1.

$\dot{V}_y$ indicates the northern acceleration, ΔA_y denotes the northern acceleration error, ε_x is the eastern gyro drift, α_0 indicates the eastern platform initial misalignment angle, α denotes the eastern platform misalignment angle, g represents the local gravitational acceleration, R is the average radius of the earth, $1/s$ denotes the integral operator, and $H_y(s)$ is the damping correction network.

The transfer function from the gyro drift ε_x to the horizontal error angle α is

$$\frac{\alpha(s)}{\varepsilon_x(s)} = \frac{s}{s^2 + \omega_s^2 \mathrm{H}_y(s)}, \tag{1}$$

where $\omega_s = \sqrt{g/R}$ is the Schuler angular frequency.

It is known from Equation (1) that the navigation system can be turned into a stable system by designing the parameters of $H_y(s)$. The principles of damping network parameter configuration are [1]

(1) The system should be stable

(2) The angular frequency of the damping should be the Schuler angular frequency ω_s

(3) The damping coefficient ξ should be set to around 0.5

(4) $H_y(s)$ should be close to 1

The parameters commonly used in a traditional second-order damping network are [8]

$$H(s) = \frac{\left(s + 8.5 \times 10^{-4}\right)\left(s + 9.412 \times 10^{-2}\right)}{\left(s + 8.0 \times 10^{-3}\right)\left(s + 1.0 \times 10^{-2}\right)}. \quad (2)$$

The parameters commonly used in a traditional third-order damping network are [26]

$$H(s) = \frac{\left(s + 8.8 \times 10^{-4}\right)\left(s + 1.97 \times 10^{-2}\right)^2}{\left(s + 4.41 \times 10^{-3}\right)\left(s + 8.8 \times 10^{-3}\right)^2}. \quad (3)$$

2.2. Traditional External Horizontal Damping Network. To compensate for the system error caused by the maneuver of the ship, the reference velocity obtained by a DVL/EML is often introduced to the navigation system. The navigation system model is shown in Figure 2.

As shown in Figure 2, the subscript c indicates that it is the system calculation result, and V_{ry} is the reference velocity obtained by DVL/EML. However, the reference velocity error δV_{ry} is also introduced into the system after introducing the reference velocity. From Figure 2, we could get the equation as follows:

$$\alpha(s) = \frac{\left[1 - H_y(s)\right]s \cdot \delta V_{ry}}{R\left[s^2 + H_y(s)\omega_s^2\right]} + \frac{\left[1 - H_y(s)\right] \cdot \delta V_{ry}(0)}{R\left[s^2 + H_y(s)\omega_s^2\right]}. \quad (4)$$

Equation (4) presents that the horizontal error angle is no longer related to the acceleration of the vehicle; it is only related to the reference velocity and $H_y(s)$. When the carrier has acceleration, the introduction of the reference velocity adds a compensation channel to the system to compensate the horizontal error angle caused by the damping network. Although the reference velocity error will affect the navigation accuracy, it is smaller than the impact of the carrier's acceleration; obviously, this method could improve the accuracy of INS.

2.3. Complementary Filtering Horizontal Damping Network [13]. In marine INS, the reference velocity is usually obtained by EML on the ship. However, the reference velocity error will change along with the ship's maneuver; sea conditions, e.g., the slope error when ship accelerates or decelerates; constant error caused by smooth delay when the ship accelerates or decelerates; constant error caused by ocean current or temperature of the sea; alternating error when the ship turns; alternating error caused by wind velocity; sinusoidal error caused by tides; and the zero-bias and random noise of the EML. Therefore, the damping network needs to have the ability to suppress these high and low frequency errors to improve the accuracy of INS.

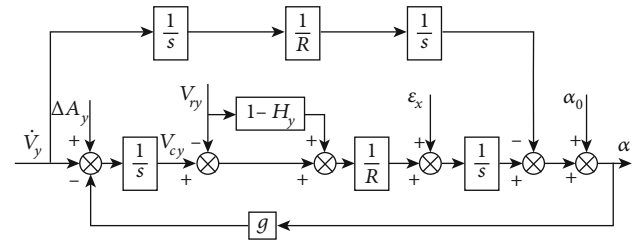

Figure 2: Block diagram of north-level correction circuit (external damping) [1].

Reference [13] proposed a novel horizontal damping network for INS based on complementary filtering. It adopted a constant velocity feedback damping network which could suppress high-frequency errors' interference effectively as A and phase lag-leading damping network which could suppress low-frequency errors' interference effectively as B. Then, the damping network A passed through a high-pass filter $1 - W(s)$, while the damping network B passed through a low-pass filter $W(s)$, the complementary filtering horizontal damping network C could be constructed by combining these two blocks. In this way, C has a good capability to suppress both high-frequency and low-frequency errors of the reference velocity.The transfer function of the complementary filtering horizontal damping network is [13]

$$H_C(s) = \frac{\left\{(1 + 2\eta + 4\zeta\eta)\omega_s s^3 + [2 + 2\zeta + 2\eta + 4\eta\zeta]\omega_s^2 s^2 + s^4 + (1 + 2\eta + 2\zeta)\omega_s^3 s + \omega_s^4\right\}}{\left\{(1 + 2\eta + 2\zeta)\omega_s s^3 + [2 + 2\zeta + 2\eta + 4\eta\zeta]\omega_s^2 s^2 + s^4 + (1 + 2\eta + 4\zeta)\omega_s^3 s + \omega_s^4\right\}}. \quad (5)$$

Here, ζ and η are two damping coefficients determining the attenuation response. The value for η has been optimized and is assigned $\eta = 0.5$ in our shipborne INS to obtain the required attenuation rate mentioned above. The analysis of the reference velocity error-induced position errors will be based on this value. Assuming $\zeta = 0.7$, the transfer function from the reference velocity error δV_{ry} to the horizontal error angle α of the complementary filtering horizontal damping network is

$$\frac{\alpha R}{\delta V_{ry}} = \frac{1.4\omega_s^3 s^2}{\left\{s^6 + 3.4\omega_s s^5 + 6.8\omega_s^2 s^4 + 8.2\omega_s^3 s^3 + 6.8\omega_s^4 s^2 + 3.4\omega_s^5 s + \omega_s^6\right\}}. \quad (6)$$

The amplitude-frequency characteristic curves of the reference velocity error to horizontal error angle of the complementary filtering horizontal damping network, the traditional second-order damping network, and the traditional third-order damping network are shown in Figure 3.

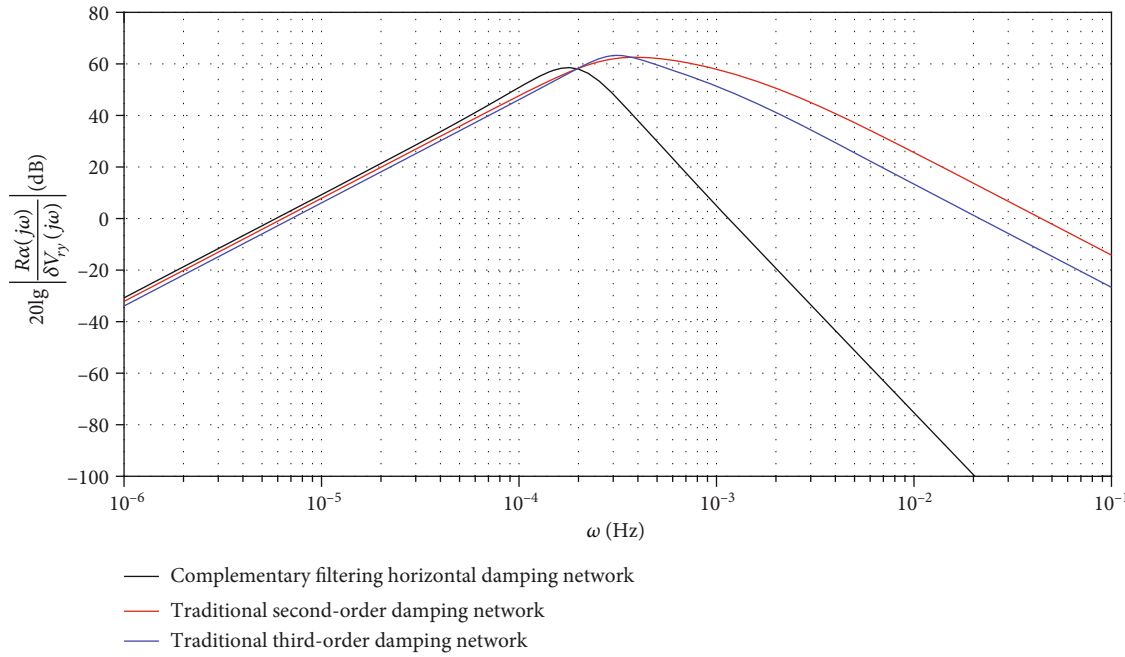

Figure 3: The amplitude-frequency characteristic curves.

Compared with other damping networks, Figure 3 demonstrates that the complementary filtering horizontal damping network has the best effect on suppressing the reference velocity errors, especially on the high-frequency reference velocity errors. It has 40 dB/10 dec or higher attenuation rate to both low-frequency and high-frequency reference velocity errors.

3. Variable Damping System Design

Although the introduction of the reference velocity will eliminate the influence of the carrier's maneuver on the system accuracy, it is inevitable to introduce reference velocity error so that it will reduce the accuracy of navigation accordingly. It is necessary to switch the damping status of INS dynamically to ensure the accuracy and stability as the change of reference velocity error. Hence, a novel variable damping system based on the variation of the reference velocity error is designed in this paper.

3.1. The Effect of Reference Velocity Error on System. The traditional external horizontal damping network is taken as an example to analyze the influence caused by the reference velocity error. Ignoring the initial error of the reference velocity, Function (4) can be converted as follows:

$$\alpha(s) = \frac{1 - H_y(s)}{R\left[s^2 + H_y(s)\omega_s^2\right]}\delta\dot{V}_{ry}(s). \tag{7}$$

Function (7) represents that the acceleration of the reference velocity error can cause a dynamic overshoot on the horizontal error angle. In the working process of INS, the dynamic overshoot is a small quantity relative to the Schuler period; in addition, the signals used in the actual system are digital signals; hence, the input of $\delta\dot{V}_{ry}$ can be regarded as pulse signals and we could obtain Function (8) by Laplace transform:

$$\delta\dot{V}_{ry}(s) = \Delta\left(\delta V_{ry}\right), \tag{8}$$

where

$$\Delta\left(\delta V_{ry}\right) = \int_{t_1}^{t_2}\delta\dot{V}_{ry}(t)dt, \tag{9}$$

where t_1 and t_2 represent two moments when the INS is working, and $t_1 < t_2$. $\Delta(\delta V_{ry})$ is the variation of the reference velocity error caused by the acceleration of the reference velocity error between these two moments.

Then, we can obtain Function (10) as follows:

$$\alpha(s) = \frac{1 - H_y(s)}{R\left[s^2 + H_y(s)\omega_s^2\right]}\Delta\left(\delta V_{ry}\right). \tag{10}$$

Function (10) indicates that the dynamic overshoot caused by the reference velocity error is proportional to the acceleration integral value of the reference velocity error, that is, proportional to the absolute value of $\Delta(\delta V_{ry})$.

To verify the results of the analysis above, the velocity error curves of INS under different reference velocity errors were investigated through simulation. The simulation assumed that the accelerometer zero-offset is 10 μg, the gyro zero-offset is 0.0001°/h, and the simulation time is 10 h. There was no reference velocity error at the initial moment, and the carrier was stationary on the external horizontal damping status in which the damping coefficient was $\zeta = 1.3$, then the

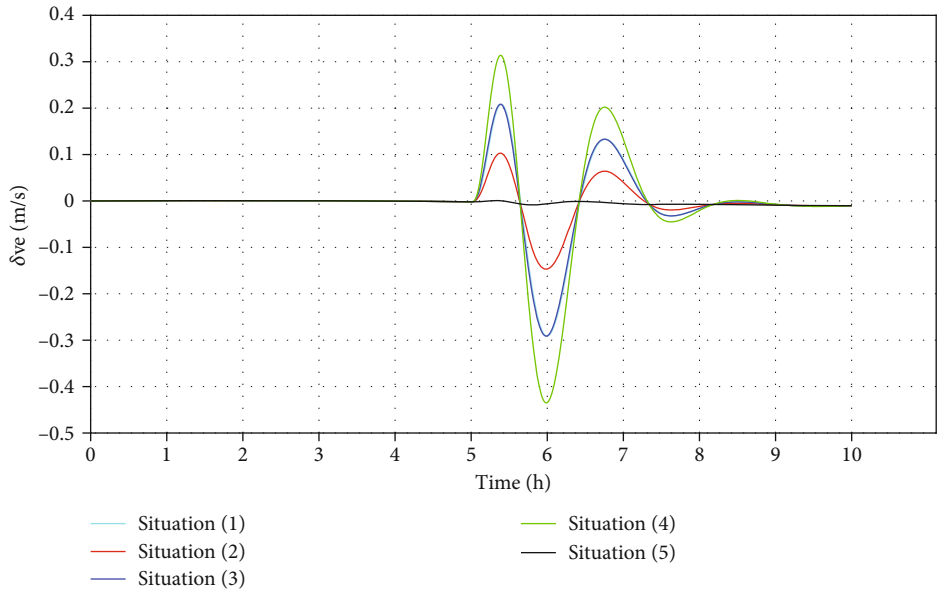

Figure 4: The eastward velocity error curves.

reference velocity error started to change at 5 h. The following situations are simulated and analyzed:

(1) The eastward reference velocity error has an acceleration of 0.01 m/s^2 for 100 s

(2) The eastward reference velocity error has an acceleration of 0.05 m/s^2 for 10 s

(3) The eastward reference velocity error has an acceleration of 0.05 m/s^2 for 20 s

(4) The eastward reference velocity error has an acceleration of 0.05 m/s^2 for 30 s

(5) The eastward reference velocity error has an acceleration of 0.01 sin $(0.2\pi t)$m/s^2 for 1000 s

Figure 4 shows the simulation results, where the blue-green line, red line, blue line, green line, and black line represent the eastward velocity error curves in the situation from (1) to (5), respectively.

It is evident that the simulation results are consistent with the above theoretical analysis. For the first and third situations, the variations of the reference velocity error are both 1 m/s although the accelerations of reference velocity errors are different. Accordingly, the overshoot errors caused by reference velocity errors are the same. For the second and fourth situations, the variations of reference velocity errors are smaller and larger than the first case, respectively, so the overshoot errors are smaller and larger than the first case correspondingly. For the fifth case, it almost does not have any overshoot error because the variation of the reference velocity error in each cycle is zero.

3.2. Selection of Damping Status Switch Method. In order to analyze the influence of damping coefficients on suppressing the reference velocity error, this paper kept the damping coefficient $\eta = 0.5$, and Function (5) can be written as follows:

$$H_C(s) = \frac{\{s^4 + 2(\zeta+1)\omega_s s^3 + (3+4\zeta)\omega_s^2 s^2 + 2(\zeta+1)\omega_s^3 s + \omega_s^4\}}{\{s^4 + 2(\zeta+1)\omega_s s^3 + (3+4\zeta)\omega_s^2 s^2 + 2(2\zeta+1)\omega_s^3 s + \omega_s^4\}}. \quad (11)$$

Because the accuracy of EML is poor when ship sails at sea, the damping coefficient ζ is usually set below 1 to get better results. Let ζ be 0.1, 0.3, 0.5, 0.7, and 0.9 and draw the amplitude-frequency characteristic curves from the reference velocity error to the horizontal error angle as in Figure 5. It presents that the ability of different damping coefficients to suppress the reference velocity error is not much different, so changing the damping coefficient has little effect on suppressing the reference velocity error. Therefore, it is suitable to switch the damping status instead of changing the damping coefficient.

The traditional variable damping method sets a reference velocity error threshold, then the system switches the damping status to undamping status when the reference velocity error reaches this error threshold. Generally, the difference between the calculated velocity of INS and the reference velocity is taken as the reference velocity error. However, in the actual navigation process at sea, the difference between the reference velocity and calculated velocity of INS will be large for a long time in some cases. Hence, if the error threshold is set too large, the traditional method is not sensitive enough to reference the velocity error so that the system cannot switch to the undamping status in a timely manner. If the error threshold is too small, it is susceptible to external interference so that the system switches the damping status frequently, which will result in a large overshoot. Besides, it may make INS on the undamping status for a long time so that the system will not be able to dampen the inertial

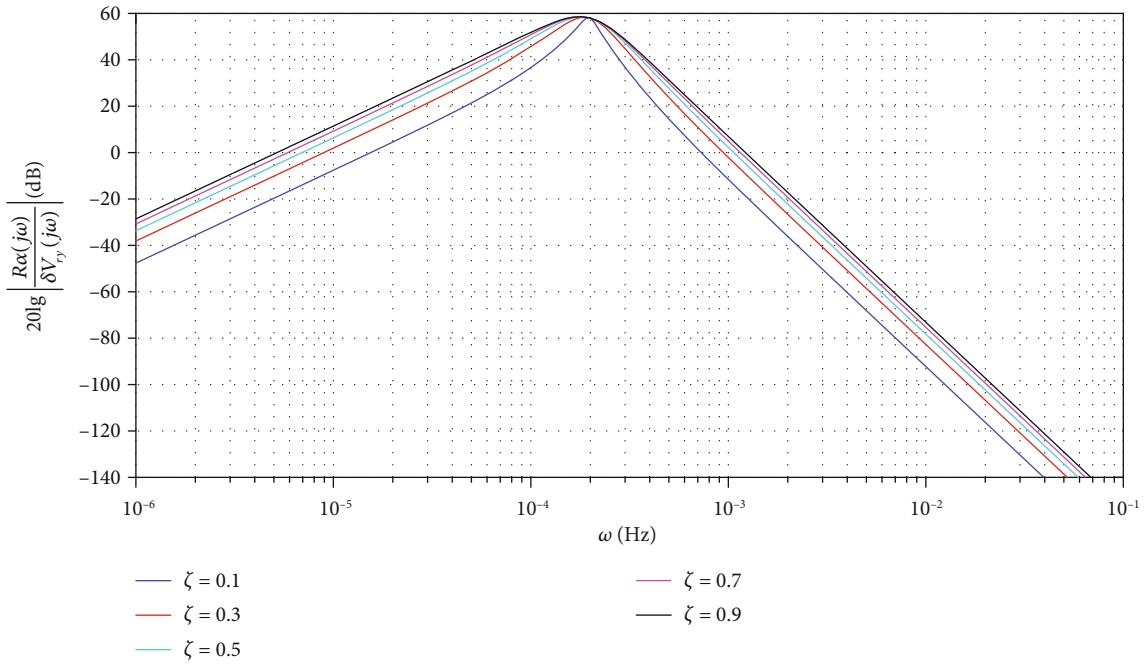

Figure 5: The amplitude-frequency characteristic curves under different damping coefficients.

navigation error caused by gyroscope drifts and other factors, resulting in the reduction of navigation accuracy. Therefore, this method is not suitable when the reference velocity error is large for a long time.

From another perspective, the reference velocity error is always large when encountering rough sea conditions or the ship turns. And the angular rate of the ship's yaw will get bigger in these conditions. According to this analysis, there is another traditional method to switch the damping status based on the change of yaw. It will switch the damping status to the undamping status when the change of yaw exceeds a specified threshold. However, this method cannot cover all situations when the reference velocity error is large such as the ship enters or exits the bay area with strong currents and cruises in rivers or straits.

On the basis of the theoretical analysis and simulation in Section 3.1, we could conclude that the navigation error caused by the reference velocity error is essentially due to the variation of the reference velocity error. In view of this analysis, this paper proposed a novel method which switches the damping status according to the variation of reference velocity error and makes the damping coefficient $\zeta = 0.5$ when the system is on damping status.

As shown in Figure 6, the proposed variable damping network added an adaptive damping module and an overshoot suppression module to the inertial navigation system loop. This method took the difference between the reference velocity and calculated velocity as the input and determined the damping status based on the input. Then, a module suppressing the overshoot caused by the damping status switch was applied to improve the navigation accuracy.

3.3. Design of Adaptive Damping Module. The variation of reference velocity error can be determined by the variation

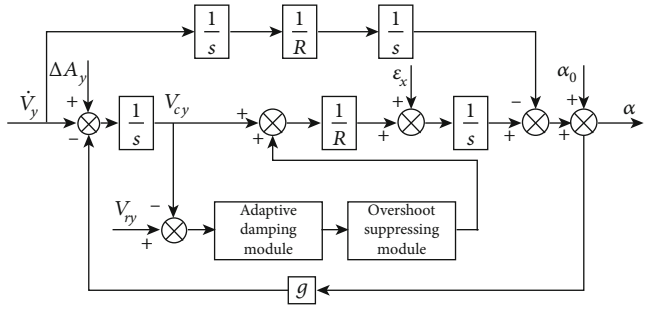

Figure 6: Block diagram of novel variable damping circuit.

of the difference between the reference velocity and calculated velocity of INS.

$$\begin{aligned} v_c &= v + dv_c, \\ v_r &= v + dv_r, \\ \delta v &= v_r - v_c = dv_r - dv_c, \end{aligned} \tag{12}$$

where v, v_c, and v_r denote the true velocity, calculated velocity, and reference velocity, respectively; dv_c and dv_r indicate the error of v_c and v_r, respectively; and δv represents the difference between calculated velocity and reference velocity.

The differences between the calculated velocity and reference velocity at times t_1 and t_2 are δv_1 and δv_2, respectively.

$$\Delta = \delta v_1 - \delta v_2 = (dv_{r1} - dv_{r2}) - (dv_{c1} - dv_{c2}). \tag{13}$$

The first term on the right side of Equation (13) is the variation of the reference velocity error, and the second term is the variation of the calculated velocity error. Because the

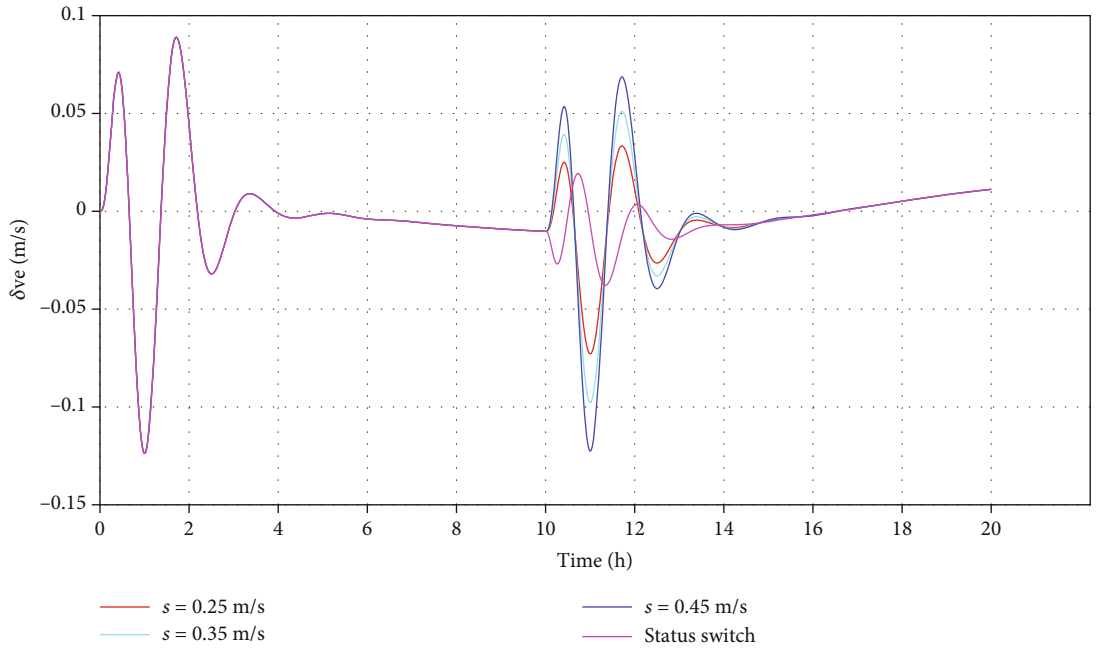

Figure 7: The overshoot errors under different situations.

calculated velocity error of the short-term has little change, when Δ is large, it can be approximately considered that Δ is the variation of reference velocity error, namely,

$$\Delta \approx dv_{r1} - dv_{r2}. \tag{14}$$

In order to eliminate the influence of transient large errors, this method took the average value of the difference between the calculated velocity and reference velocity over a period of time. Then, this method chose a suitable time duration to calculate the variation of reference velocity error based on the principle of window detection [33]. The variation of the reference velocity error can be described by the formula as follows:

$$s = \left| \frac{\sum_{i=t-n}^{i=t} (v_{ri} - v_{ci})}{n} - \frac{\sum_{i=t-t_0-n}^{i=t-t_0} (v_{ri} - v_{ci})}{n} \right|, \tag{15}$$

where n is the time length of taking the average value; t and t_0 represent the current moment and the width of the window, respectively; v_{ci} and v_{ri} denote the calculated velocity of INS and the reference velocity at the moment of i, respectively; and s indicates the absolute variation value of the reference velocity error from the moment of $i = t - t_0$ to $i = t$. According to the accuracy of our EML and sea trial, the time length of taking the average value was determined to be 20, that is, $n = 20$. The damping status should be switched at the moment when the value of s exceeds the certain threshold.

There is a contradiction in the design of the damping status switch based on the principle of window detection, that is, the wider the window is and the lower the misjudgment rate of the reference velocity error is, the longer the time lag is. Therefore, the width of the window needs to be set according to both the misjudgment rate and the time lag. In addition, the width also needs to be determined according to the threshold of s.

Besides, the switch of the damping status will lead to the overshoot error of INS; thus, it is necessary to weigh the overshoot error caused by the switch of the damping status and the oscillation error caused by the reference velocity error when designing the basis for the damping status switch.

To select the appropriate values of the width and threshold of s, the velocity error curves of the INS under different s and the situation when the status switches were investigated through simulation. In the sea trial environment, the reference velocity error always exists and maintains a large order of magnitude. According to the accuracy of EML used in our sea trial, the average value of the reference velocity error can be taken as 0.5 m/s. The simulation assumed that the accelerometer zero-offset is 10 μg, the gyro zero-offset is 0.0001°/h, and the simulation time is 20 h. There was a 0.5 m/s reference velocity error at the initial moment, and the carrier was stationary on the external horizontal damping status in which the damping coefficient was $\zeta = 0.5$, then a different s started to appear or the status switched to the undamping status for 200 s at 10 h.

In Figure 7, "$s = 0.25$ m/s," "$s = 0.35$ m/s," and "$s = 0.45$ m/s" indicate that the variation of the reference velocity error is 0.25 m/s, 0.35 m/s, and 0.45 m/s at the moment of 10 h, respectively. The curve of the "status switch" indicates that the system switches the status from the damping status to the undamping status at the moment of 10 h and the reference velocity error maintains the same. Figure 7 shows that the overshoot error when $s = 0.25$ m/s is approximately equal to the overshoot error when the status switches to the undamping status so that the system should not switch the damping status when $s < 0.25$ m/s.

Besides, if the value of s falls near the boundary point, the phenomenon of the frequent damping status switch will

occur, which maybe result in an error jump. Hence, changing the system damping status frequently is undesirable so that a fuzzy controller was designed in this paper. The fuzzy controller took s as the input and the system damping status as the output.

In our sea trial, the variation of the reference velocity error may fluctuate from 0 to 0.4 m/s in a short time ($t < 100$ s) due to the influence of sea waves and other factors. In this situation, the overshoot will be larger if the damping status switches. In addition, the accuracy of EML used in our sea trial is poor. Therefore, the original reference velocity obtained by EML is smoothed, and the fluctuation amplitude of the processed reference velocity is 0.1 m/s. In order to avoid the misjudgment and frequent switch caused by these factors above, the variation of the reference velocity error was divided into three cases: large, medium, and small. The degree of membership function of the fuzzy controller was designed as shown in Figure 8.

Based on the previous analysis, the appropriate parameters of the fuzzy controller were determined as follows:

$$\begin{aligned} a &= 0.25 \text{ m/s}, \\ b &= 0.35 \text{ m/s}, \\ c &= 0.45 \text{ m/s}. \end{aligned} \tag{16}$$

The statuses of the output variable y and their representative meanings are as follows:

(1) $y = f_1$ means that $s \le a$; the current variation of the reference velocity error is small so the system should be on damping status

(2) $y = f_2$ means that $a < s < c$; the system should maintain the current status

(3) $y = f_3$ means that $s \ge c$; the current variation of the reference velocity error is large, and the system should be on undamping status

The reference velocity error is mainly caused by the acceleration and deceleration of the ship. When the ship accelerates or decelerates, the EML will produce an error component which is directly proportional to the ship's acceleration due to its own characteristics. Generally speaking, the variation of the reference velocity error needs 80 s to reach 0.5 m/s in our sea trial when the ship accelerates or decelerates. Considering these factors above, the window width was assigned 80 s, that is, $t_0 = 80$.

Figure 9 shows the schematic diagram of the damping status switch, where f indicates the output of the degree of membership function and i represents the current system

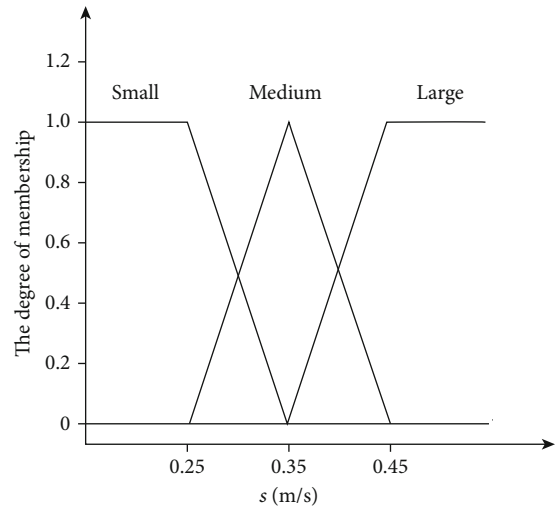

Figure 8: Degree of membership function.

damping status. The switch process can be expressed as follows:

(1) Calculating the current value of s according to Equation (15)

(2) The value of s is sent to the degree of membership function and gets the output status f

(3) In order to avoid frequent switching of the damping status, it is stipulated that the system damping status is switched when the output status f is not f_2 and it is different from the current system damping status for 20 consecutive times. Otherwise, the system maintains the current status, and the value of m is reset to zero or plus one according to the status of f, then performs the next round of calculations

3.4. The Method of Overshoot Suppression. The switch of the damping status will break the balance and cause overshoot error. In consideration of this condition, it is necessary to take measures to restrain this overshoot. First of all, in order to realize the calculation of the damping network in a digital computer, the equivalent discretization of the analog damping network is required. There are some methods to the discrete transfer function, such as backward difference method, zero-order/first-order hold method, impulse response invariant method, and bilinear transformation method. In order to ensure single-value mapping and avoid frequency aliasing, this paper chose the bilinear transformation method to discretize the damping network. In addition, the method of ω_s precorrection was applied to overcome a nonlinear distortion of frequency. Let $Q(s) = 1 - H_C(s)$, the discretization result of $Q(s)$ can be obtained as follows:

$$Q(z) = Q(s)\Big|_{s=\frac{\omega_s}{\tan(\omega_s T/2)}\frac{1-z^{-1}}{1+z^{-1}}} = \frac{2\zeta u\left(1 + 2z^{-1} - 2z^{-3} - z^{-4}\right)}{\left\{u^4 + 2d_1 + d_2 + 2d_3 + 1 - 4(u^4 + d_1 - d_3 - 1)z^{-1} + 2(3u^4 - d_2 + 3)z^{-2} - 4(u^4 - d_1 + d_3 - 1)z^{-3} + (u^4 - 2d_1 + d_2 - 2d_3 + 1)z^{-4}\right\}}, \tag{17}$$

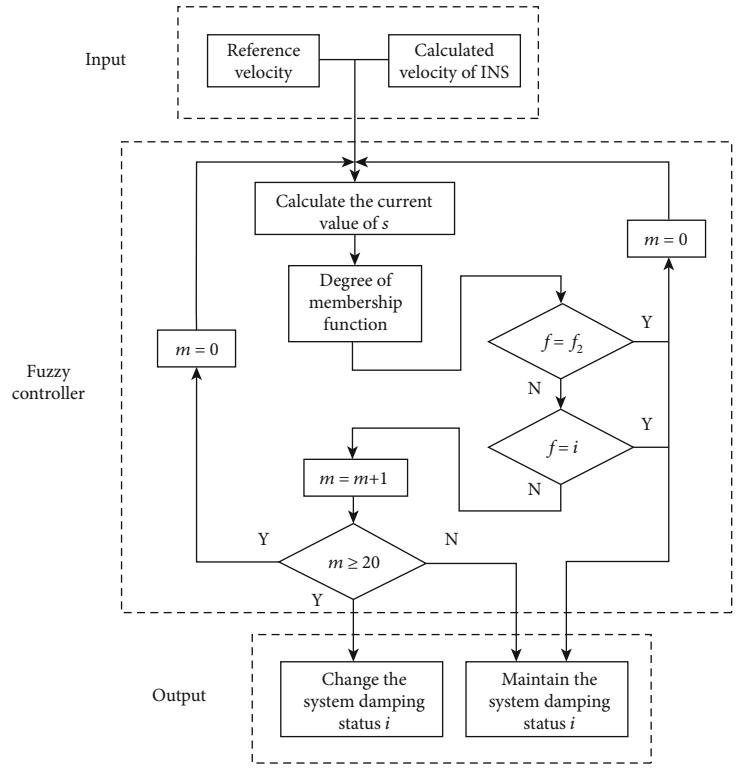

Figure 9: Flow chart of damping status switch.

where T is the discretization interval and is set to 1 s here. And

$$\begin{aligned} u &= \frac{1}{\tan(\omega_s T/2)}, \\ d_1 &= (1+\zeta)u^3, \\ d_2 &= (3+4\zeta)u^2, \\ d_3 &= (2\zeta+1)u. \end{aligned} \tag{18}$$

Then, there is

$$\begin{aligned} (u^4 + 2d_1 + d_2 + 2d_3 + 1)c_k = {} & 4(u^4 + d_1 - d_3 - 1)c_{k-1} - 2(3u^4 - d_2 + 3)c_{k-2} \\ & + 4(u^4 - d_1 + d_3 - 1)c_{k-3} \\ & - (u^4 - 2d_1 + d_2 - 2d_3 + 1)c_{k-4} \\ & + 2\zeta u(r_k + 2r_{k-1} - 2r_{k-3} - r_{k-4}), \end{aligned} \tag{19}$$

where c_k is the damping correction signal at the current moment in the local horizontal coordinate system and r_k is the difference between the reference velocity and the calculated velocity of INS, which represents the reference velocity error.

Because the magnitude of the overshoot error is positively related to the variation of the damping coefficient when the system damping status is switched, so the value of the damping coefficient should gradually increase from zero to the target value when the system switches from the undamping status to the damping status. When the system switches from the damping status to the undamping status, the system should switch to the undamping status to avoid the influence of the reference velocity error in time. In addition, the damping correction signal should remain unchanged when the system damping status switches, so as to avoid the overshoot error becoming larger due to the sudden disappearance of the damping correction signal.

Considering the transfer function calculation process after discretization, this paper adopted the following measure to suppress the overshoot of the damping switch. Figure 10 shows the schematic diagram of the overshoot suppression, where e indicates the Euler number, ξ is the target value of the damping coefficient, and ζ is the actual damping coefficient used in the calculation.

The overshoot suppressing process can be expressed as follows.

When the damping status of the system switches,

(a) The damping status of the system switches from the undamping status to the damping status; the initial value of each integrator of the damping network is cleared to zero, that is, $c_{k-1} = c_{k-2} = c_{k-3} = c_{k-4} = 0$ and $r_{k-1} = r_{k-2} = r_{k-3} = r_{k-4} = 0$. Then, let the damping coefficient ζ gradually increase from zero to the target value ξ in the form of an exponential function in 50 s. For example, at the moment of switching, the value of ζ is set to $\xi \times e^{-49}$; then in the next calculation after switching the damping status, the value of ζ is set to $\xi \times e^{-48}$; next, the value of ζ is set to $\xi \times$

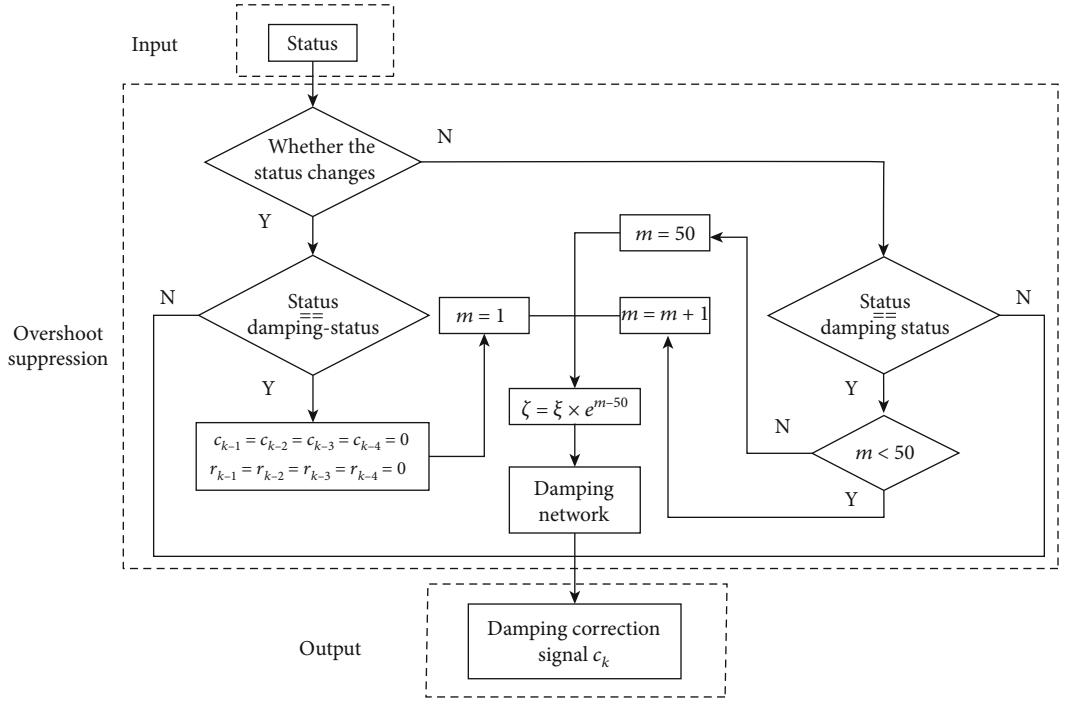

Figure 10: Flow chart of overshoot suppressing.

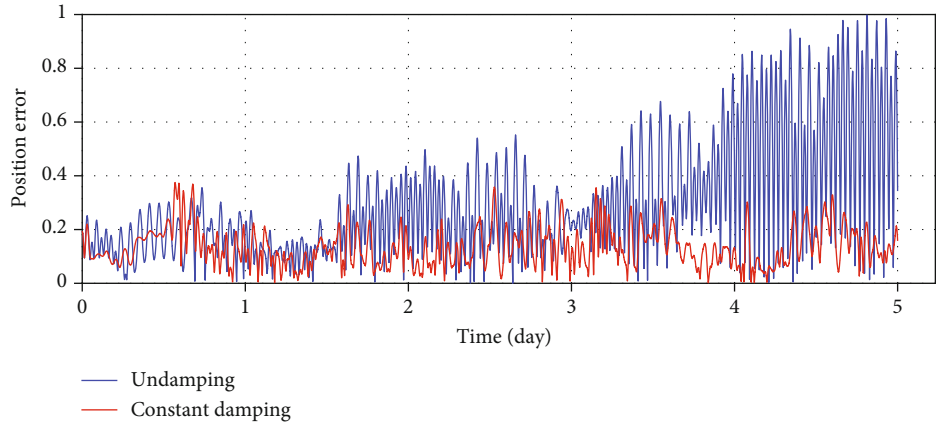

Figure 11: Position error curves of undamping and damping networks.

e^{-47}, and so on. Finally, the value of ζ is set to $\xi \times e^{-0} = \xi$

(b) The damping status of the system switches from the damping status to the undamping status; the damping network is shielded, while the damping correction signal c_k remains the same instead of shielding the damping correction signal

When the damping status of the system does not switch,

(a) The system maintains the damping status; if the value of m is less than 50, it means the system is still in the process of switching from the undamping status to the damping status, and the value of the damping coefficient ζ gradually increase to the target value ξ in the form of an exponential function. If the value of m is not less than 50, the value of the damping coefficient ζ is equal to ξ

(b) The system maintains the undamping status; the damping network is shielded, while the damping correction signal c_k remains the same

4. Simulation Results and Discussion

In order to prove the effectiveness of this method described in the previous section, marine data simulation experiments were carried out in the VC environment. Besides, this paper verified the superiority of the proposed method by comparing with the undamping system, constant damping system, and traditional variable damping system based on the yaw of the ship which is described in Section 3.2.

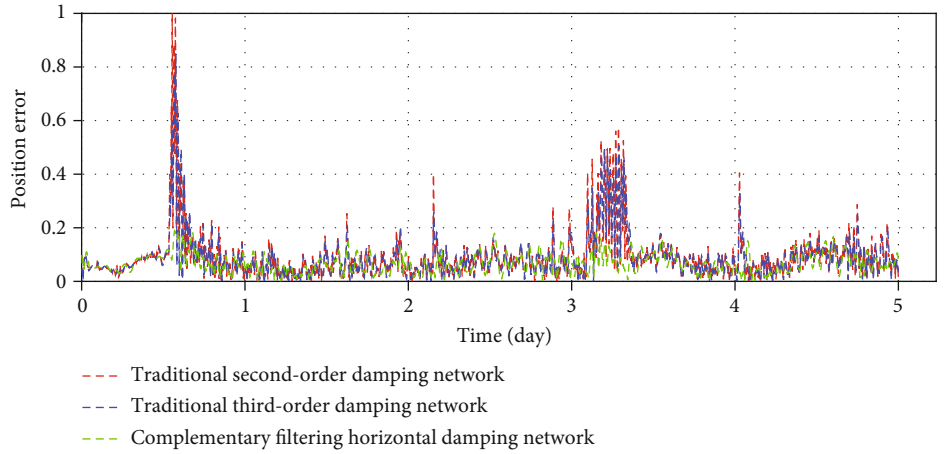

Figure 12: Position error curves of different damping networks.

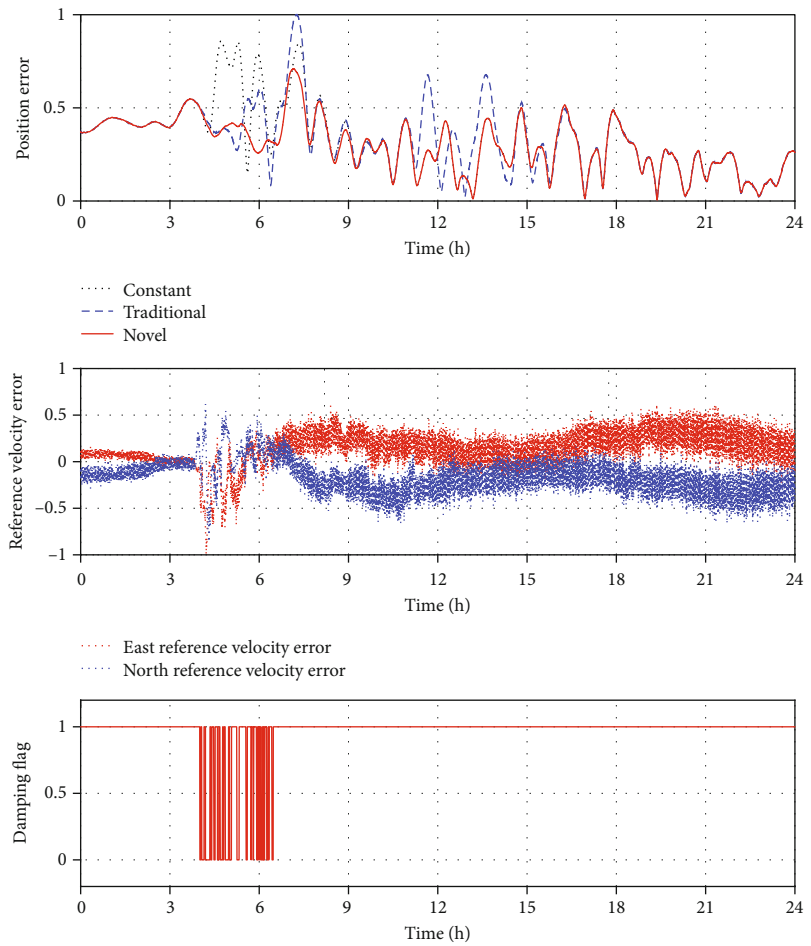

Figure 13: Simulation Experiment I.

Abundant data from a shipborne INS collected during an actual sea test were taken to be simulated in this paper. The shipborne INS had two dual-axis gyros with ultralow drift and three orthogonal pendulous accelerometers which are mounted on a gyrostabilized gimbaled platform. An altimeter and an EML were used to provide the altitude and

Table 1: RMSEs of each damping network.

No.	4-8 h	11-15 h
Constant	0.4961	0.2320
Traditional	0.4288	0.3163
Novel	0.3497	0.2318

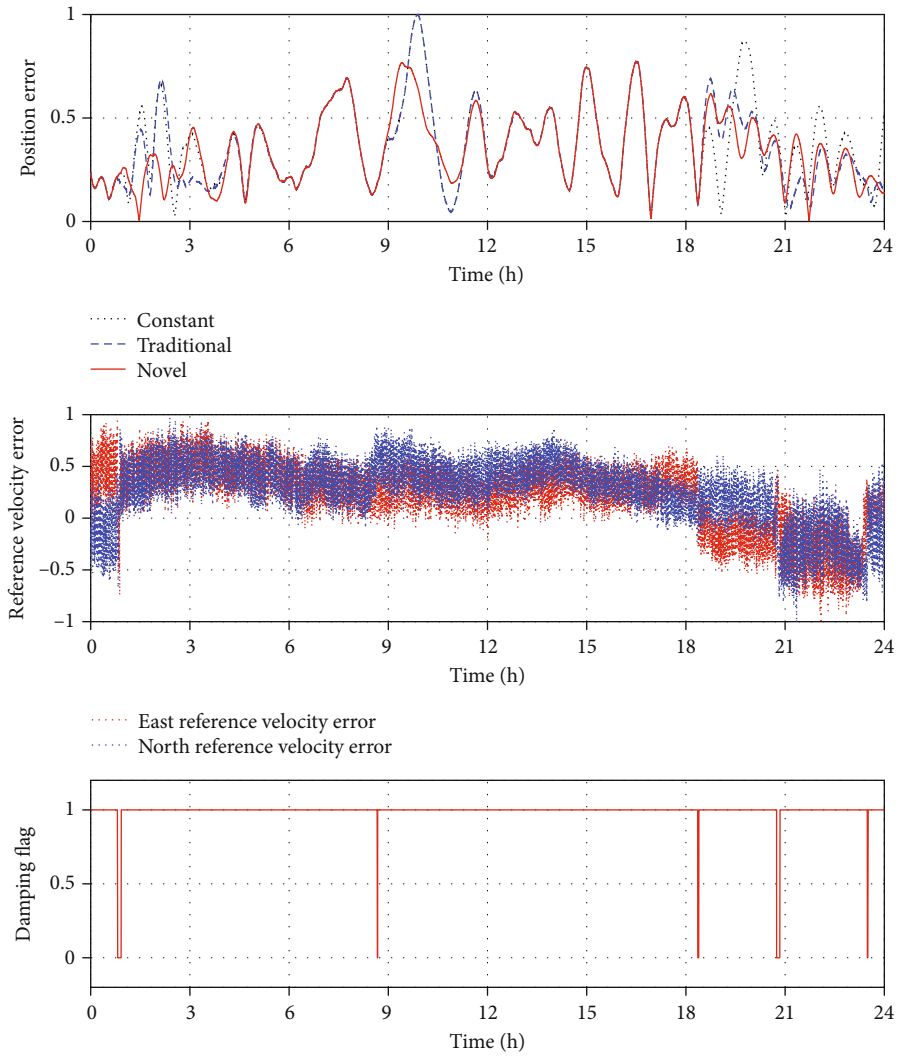

Figure 14: Simulation Experiment II.

reference velocity for the damping of the vertical and horizontal channels, respectively.

The calculated position information of INS is compared with the outputs of a GPS to obtain the position error. The velocity information of the EML is compared with the outputs of a GPS to obtain the reference velocity error. A damping flag indicates the situation of the damping switch when using the novel method proposed in this paper. When the damping flag is 0, the system is on the undamping status. When the damping flag is 1, the system is on the damping status. Besides, all experimental results are normalized in this paper.

First, the data of the first five days were taken to simulate the undamping and constant damping inertial navigation systems. The position error curves are shown in Figure 11. It shows that the position error of the undamping system is divergent with the increase of time, while the position error of the constant damping system does not diverge. In addition, the traditional second-order damping network and traditional third-order damping network INS data will also be displayed to compare with the complementary filtering horizontal damping network. Figure 12 shows that the accuracy of the complementary filtering horizontal damping network is the best.

Table 2: RMSEs of each damping network.

No.	1-4 h	9-11 h	18-24 h
Constant	0.2358	0.4042	0.2733
Traditional	0.2117	0.4042	0.2415
Novel	0.1659	0.3616	0.2371

4.1. Simulation Experiment I. In Experiment I, data for the first day during this sea test were taken to be simulated. The sea test had an initial position error, then the ship started to maneuver and the reference velocity error appeared. The position error curves, reference velocity error curves, and damping flag plot when using the novel variable damping network are shown in Figure 13.

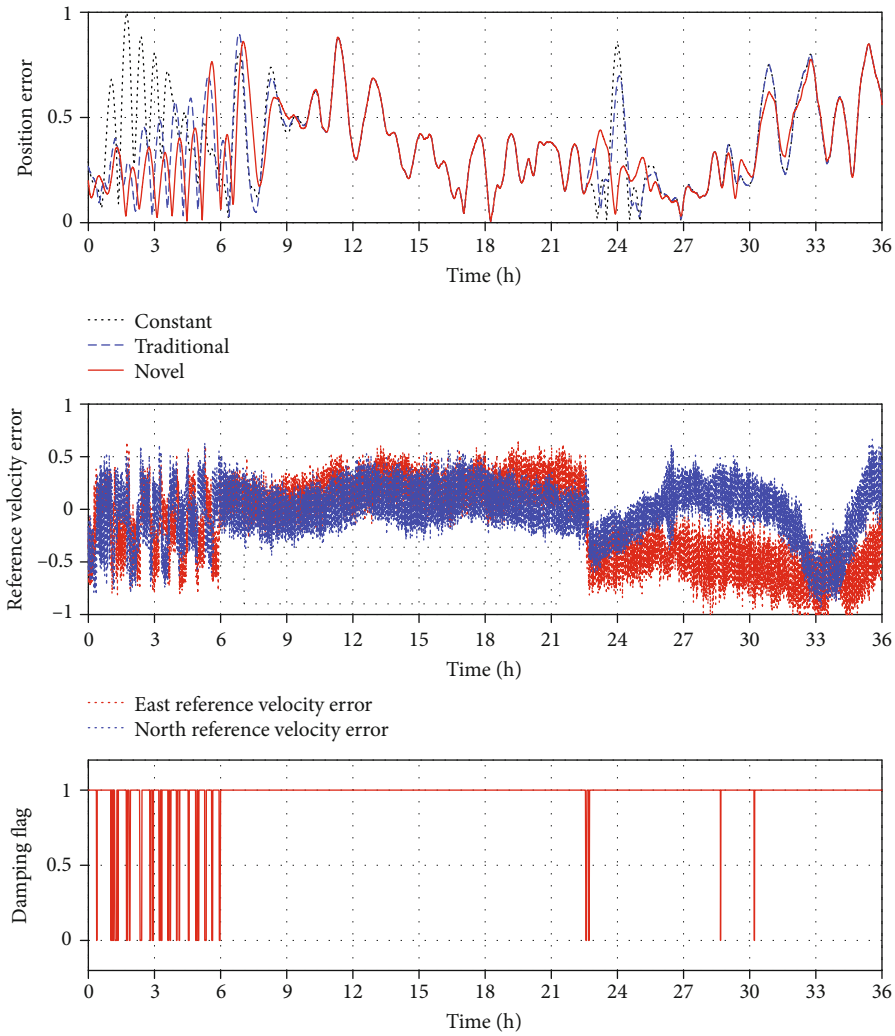

Figure 15: Simulation Experiment III.

The root mean square errors (RMSEs) of each damping network, which evaluate the accuracy of the navigation position, are listed in Table 1.

Figure 13 shows that both the traditional variable damping system and the novel variable damping system can switch to the undamping status to reduce the position error when the variation of the reference velocity error is high. However, the position error of the novel system is smaller than that of the traditional system, which indicates that the module of the overshoot suppression can restrain the overshoot error of the damping switch. The 11-15 h segment of Figure 13 shows that the position error of the traditional system increased; the reason is that the system switched the damping status due to the wrong judgement.

4.2. Simulation Experiment II. In Experiment II, data for the third day during this sea test were taken to be simulated. The position error curves, reference velocity error curves, and damping flag plot are shown in Figure 14.

The RMSEs of each damping network are listed in Table 2.

Table 3: RMSEs of each damping network.

No.	0-6 h	22-25 h	28-32 h
Constant	0.3391	0.2471	0.2560
Traditional	0.2362	0.2276	0.2559
Novel	0.2015	0.1829	0.2429

Figure 14 shows that the ability of the overshoot suppression of the novel variable damping system is stronger than that of the traditional variable damping system. The 9-12 h segment of Figure 14 shows that the position error of the traditional system is the same as the constant damping system, which indicates that the traditional system did not change the damping status.

4.3. Simulation Experiment III. In Experiment III, 1.5 days of data during this actual sea test were taken to be simulated. The position error curves, reference velocity error curves, and damping flag plot are shown in Figure 15.

The RMSEs of each damping network are listed in Table 3.

We can find that the ability of the overshoot suppression of the novel variable damping system is stronger than that of the traditional variable damping system; thus, the novel system has the highest navigation accuracy.

4.4. Analysis. As shown in Figure 11, the undamping navigation system is not stable and its position information will diverge with time. Figure 12 shows that the accuracy of the complementary filtering horizontal damping network is the best. Figures 13–15 indicate that the novel variable damping system will switch from the external horizontal damping status to the undamping status in a timely manner when the reference velocity error changes. In this way, the position error can be suppressed to a smaller extent, and the maximum position error is reduced compared with the constant damping system and traditional variable damping system, which indicates that the navigation accuracy of the novel variable damping system is the best. Because it is difficult to obtain the accurate reference velocity during the sea test, the credible velocity error curves are not given here. But for a system with horizontal velocity damping, the velocity error can be approximated as the first-order differential of the position error. Therefore, the simulation results can confirm that the velocity accuracy of the novel variable damping system is the best.

5. Conclusions

Aiming to address the problem that the navigation accuracy of the constant damping system is sensitive to the error of the reference velocity, and switching the damping status will lead to a large overshoot error, a variable damping INS for ships based on the variation of the reference velocity error is proposed. In order to adapt to the long-term large amplitude of the reference velocity error when the sea condition is poor, this proposed method switches the damping status according to the variation of the reference velocity error. First, the principle of window detection is adopted to design the damping switch basis to obtain the suitable damping status. Besides, a fuzzy controller is used to avoid the system switching frequently between damping status and undamping status. In addition, a design of the overshoot suppression is applied to suppress the overshoot caused by the damping status switch. Compared with the undamping system, constant damping system, and traditional variable damping system, simulation experiments verified that the novel variable damping system which is proposed in this paper can attenuate the error caused by the reference velocity error most effectively. In conclusion, it has high significance on the occasions when the reference velocity error maintains a large amplitude for a long time and has certain engineering application value.

Data Availability

The initial data of the sea test used to support the findings of this study are available from the corresponding author upon request.

Conflicts of Interest

The authors declare that there is no conflict of interest regarding the publication of this paper.

Acknowledgments

The authors would like to acknowledge the support offered by the following program: National Natural Science Foundation of China (62073184).

References

[1] Z. Y. Gao, *Inertial Navigation System Technology*, Tsinghua University Press, Beijing, China, 2012.

[2] D. A. Tazartes, "Inertial navigation: from gimbaled platforms to strapdown sensors," *IEEE Transactions on Aerospace and Electronic Systems*, vol. 47, pp. 2292–2299, 2011.

[3] K. R. Britting, *Inertial Navigation Systems Analysis*, John Wiley & Sons, Inc., New York, NY, USA, 1971.

[4] Y. B. Chen and B. Zhong, *Principles of Inertial Navigation*, National Defense Industry Press, Beijing, China, 2007.

[5] D. H. Titterton and J. L. Weston, *Strapdown Inertial Navigation Technology*, AIAA, Washington, DC, USA, 2nd edition, 2004.

[6] D. M. Huang, S. X. Zhang, and F. Sun, *Gyrocompass*, National Defence Industry Press, Beijing, China, 1990.

[7] W. Gao, Y. Zhang, B. Xu, and Y. Y. Ben, "Analyse of damping network effect on SINS," in *2009 International Conference on Mechatronics and Automation*, pp. 2530–2536, Changchun, China, August 2009.

[8] F. J. Qin, A. Li, and J. N. Xu, "Improved internal damping method for inertial navigation system," *Journal of Chinese Inertial Technology*, vol. 21, pp. 147–154, 2013.

[9] K. Tang, J. Wang, W. Li, and W. Wu, "A novel INS and Doppler sensors calibration method for long range underwater vehicle navigation," *Sensors*, vol. 13, no. 11, pp. 14583–14600, 2013.

[10] I. Klein and R. Diamant, "Observability analysis of DVL/PS aided INS for a maneuvering AUV," *Sensors*, vol. 15, no. 10, pp. 26818–26837, 2015.

[11] D. Johnson and S. Eppig, "Aided inertial navigation systems for underwater vehicles," in *Proceedings of the 1987 5th International Symposium on Unmanned Untethered Submersible Technology*, pp. 265–282, Durham, NH, USA, June 1987.

[12] J. F. Kasper and R. A. Nash, "Doppler radar error equations for damped inertial navigation system analysis," *IEEE Transactions on Aerospace and Electronic Systems*, vol. AES-11, no. 4, pp. 600–607, 1975.

[13] Q. E. He, Z. Y. Gao, Q. P. Wu, and W. Q. Fu, "Design of horizontal damping network for INS based on complementary filtering," *Journal of Chinese Inertial Technology*, vol. 20, pp. 157–161, 2012.

[14] W. Huang, T. Fang, L. Luo, L. Zhao, and F. Che, "A damping grid strapdown inertial navigation system based on a Kalman filter for ships in polar regions," *Sensors*, vol. 17, no. 7, p. 1551, 2017.

[15] F. Liu, C. Liu, H. N. Weng, and X. M. Hu, "Level damping algorithm of SINS based on Kalman filtering," *Journal of Chinese Inertial Technology*, vol. 3, pp. 285–288, 2013.

[16] L. Feng, Z. H. Deng, B. Wang, and S. T. Wang, "Absolute velocity damping algorithm with varying damping ratio for inertial navigation systems based on Kalman filter," in *Proceedings of 2016 IEEE Chinese Guidance, Navigation and Control Conference*, pp. 2461–2466, Nanjing, China, August 2016.

[17] M. Karimi, M. Bozorg, and A. R. Khayatian, "A comparison of DVL/INS fusion by UKF and EKF to localize an autonomous underwater vehicle," in *Proceedings of the 2013 First RSI/ISM International Conference on Robotics and Mechatronics (ICRoM)*, pp. 62–67, Tehran, Iran, 2013.

[18] J. H. He, "INS/GPS/EM-LOG integrated navigation system technology," Master thesis, Harbin Engineering University, Harbin, China, 2019.

[19] X. Yan, Y. Yang, Q. Luo, Y. Chen, and C. Hu, "A SINS/DVL integrated positioning system through filtering gain compensation adaptive filtering," *Sensors*, vol. 19, no. 20, p. 4576, 2019.

[20] A. Tal, I. Klein, and R. Katz, "Inertial navigation system/Doppler velocity log (INS/DVL) fusion with partial DVL measurements," *Sensors*, vol. 17, no. 2, p. 415, 2017.

[21] F. Zha, F. J. Qin, F. Li, and B. Ye, "Fast external damping algorithm of inertial guidance system under external velocity reference condition," *Journal of Wuhan University*, vol. 44, no. 3, pp. 398–404, 2019.

[22] I. A. Mandour and M. M. El-Dakiky, "Inertial navigation system synthesis approach and gravity-induced error sensitivity," *IEEE Transactions on Aerospace and Electronic Systems*, vol. 24, no. 1, pp. 40–50, 1988.

[23] W. Q. Huang, Y. L. Hao, J. H. Cheng, G. Li, J. G. Fu, and X. B. Bu, "Research of the inertial navigation system with variable damping coefficients horizontal damping networks," in *Proceedings of the MTTS/IEEE Techno-Ocean'04*, pp. 1272–1276, Kobe, Japan, November 2004.

[24] B. Xu and F. Sun, "An independent damped algorithm based on SINS for ship," in *Proceedings of the 2009 International Conference on Computer Engineering and Technology*, pp. 88–92, Singapore, January 2009.

[25] L. Jiang, Y. Z. Yu, and Y. Chen, "An adaptive-damping network designed for inertial navigation system of ships," *Electro-Optical & Control*, vol. 4, pp. 52–55 + 96, 2014.

[26] J. Sun, X. Xu, Y. Liu, T. Zhang, Y. Li, and J. Tong, "An adaptive damping network designed for strapdown fiber optic gyrocompass system for ships," *Sensors*, vol. 17, no. 3, p. 494, 2017.

[27] P. Yu and G. L. Yang, "An adaptive level damped algorithm based on PINS for ship," *Advanced Materials Research*, vol. 2542, pp. 2162–2166, 2013.

[28] H. Y. He, J. N. Xu, and F. J. Qin, "Research for SINS damping overshoot error suppression algorithm," *Ship Electronic Engineering*, vol. 11, pp. 39–41, 2012.

[29] K. Li, J. J. Zhang, and F. Liu, "A fuzzy control internal damping algorithm in a long-endurance inertial navigation system," *Journal of Harbin Engineering University*, vol. 4, pp. 485–488, 2012.

[30] F. J. Qin, A. Li, J. N. Xu, and F. Zha, "Horizontal inner damping method with continuously adjustable parameter for inertial navigation system," *Journal of Chinese Inertial Technology*, vol. 3, pp. 290–293, 2012.

[31] A. V. Chernodarov, "Adaptive robust damping of divergent oscillations in updatable inertial systems," in *Proceedings of the 2nd International Conference*, pp. 133-134, St. Petersburg, Russia, July 2000.

[32] W. R. Liu and L. J. Zhuang, "Adaptive control of horizontal damping network of inertial navigation system," *Journal of Tianjin University*, vol. 2, pp. 146–149, 2005.

[33] L. Feng, "Research on damping and comprehensive calibration techniques for long-term inertial navigation systems," PhD thesis, Beijing Institute of Technology, Beijing, China, 2016.